

## INSTABILITY OF LONGITUDINAL DISTRIBUTION OF FLUVIAL BED-SURFACE COMPOSITION

By

Tetsuro TSUJIMOTO

Department of Civil Engineering, Kanazawa University  
2-40-20, Kodatsuno, Kanazawa, 920, Japan

### ABSTRACT

Spatially cyclic patterns of sorting (longitudinal alternation of the coarser and the finer parts of the bed surface) are often observed in a stream composed of sand and gravel. Such variability is termed "longitudinally alternate sorting" and is regarded as a result of an instability of bed-surface composition due to selective bed-load transport for each grain size of the sediment mixture. The formation mechanism of longitudinally alternate sorting is formulated as a linear instability problem with a specially prepared non-equilibrium bed-load transport law for graded materials characterized by pick-up rate and step length for each grain size. For simplicity, the analysis is conducted for an idealized mixture composed of two typical sizes: sand and gravel. The theory demonstrates the possibility of formation of longitudinal wavy pattern of sorting propagating downstream. The maximum growth rate defines a predominant alternation of sorting, and the wave length and the propagation celerity of the alternate sorting are predicted.

### INTRODUCTION

In a stream composed of sand and gravel, several kinds of sorting are observed. Typical examples are armor coat and pavement formations. Besides these "monotonous" processes, "wavy" patterns of sorting are also observed. In other words, stripes due to longitudinal alternation of sorting or lateral alternation of sorting are often observed in fluvial streams. The bed with the longitudinal alternation of sorting is observed (as reported by Ikeda & Iseya (3) and Kuhnle & Southard (5)). The lateral alternation of sorting is constituted by "longitudinal sorting stripes" (10). These alternate sorting processes are interesting not only from the viewpoint of river morphology but also from that of river engineering because they cause considerable fluctuation of sediment transport. These phenomena might be regarded as instability of bed-surface composition due to sorting process inherent to non-equilibrium transport of heterogeneous size bed material.

Figure 1 demonstrates the "longitudinally alternate sorting" observed in the flume by Ikeda & Iseya (3), and Fig.2 shows that the fractional bed-load transport rates fluctuate with different phase shifts. Kuhnle & Southard (5) observed these longitudinally alternate sortings in a gravel-bed flume and thus they used the term "gravel sheet," but the experiments by Ikeda & Iseya (3) revealed that such a sorting could be observed in a bed composed of coarse and fine sand as well as in a bed composed of gravel and sand.

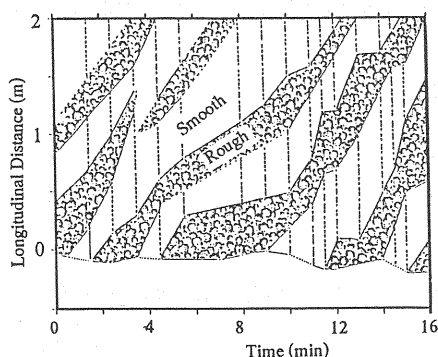


Fig.1 Illustration of longitudinally alternate sorting( from Ikeda & Iseya's experiment)

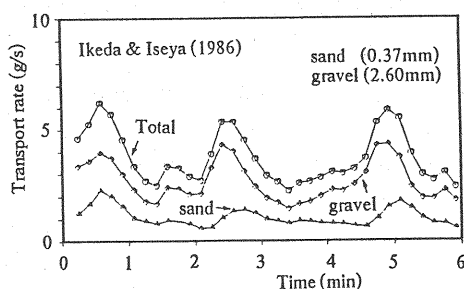


Fig.2 Fluctuation of fractional bed-load discharge (Ikeda & Iseya)

The formation of such a longitudinally alternate sorting might be treated as a problem of longitudinal instability for the volumetric ratio of gravel to the total bed materials in the surface-layer of the bed. Study of the formation of small scale sand waves has developed since Kennedy's epoch-making work (4) where he introduced linear instability analysis. Instead of bed elevation, the bed-surface composition is focussed here. By applying a linear instability analysis, the criterion of instability and the propagation celerity of disturbance of bed-surface composition are clarified in this paper. Furthermore, several data observed in flume and stream are discussed in comparison with the analytical results.

### BED-LOAD TRANSPORT OF GRADED MATERIAL

It is necessary to describe non-equilibrium transport process of graded bed material properly in order to explain an instability of bed-surface composition, as expected from the fact that a sand bed instability as formation mechanism of small scale bed-forms is caused by a lag of bed-load motion due to non-equilibrium properties (6). Because a sorting process should be described simultaneously with the transport process for the present topic, a transport model for each grain size is needed. A bed-load transport model characterized by pick-up rate and step length for each grain size (7) is a powerful means.

When the volumetric ratio of the  $i$ -th fraction material with the diameter  $d_i$  to the total bed materials in the bed-surface layer is represented by  $p_i$ , the volume of the  $i$ -th fraction dislodged from the bed per unit area per unit time,  $E_i(x,t)$ , is expressed as follows by using the pick-up rate of the  $i$ -th fraction of the sediment mixture,  $p_{si}$ :

$$E_i(x,t) = V_i(x,t) \cdot p_{si}(x,t) = V \cdot p_i(x,t) \cdot p_{si}(x,t) \quad (1)$$

in which  $V_i$ =substantial volume of sediment particles of the  $i$ -th fraction in the bed-surface layer per unit area;  $V$ =total of  $V_i$  ( $V=(1-\rho_0)\theta_E$ ;  $\theta_E$ =thickness of the surface layer; and  $\rho_0$ =porosity of bed material).

The non-equilibrium transport rate of the  $i$ -th fraction,  $q_{Bi}(x,t)$ , is expressed as follows:

$$q_{Bi}(x,t) = \int_0^{\infty} E_i(x-\xi,t) \int_{\xi}^{\infty} f_{Xi}(\zeta) d\zeta d\xi \quad (2)$$

in which  $x$ =longitudinal distance;  $t$ =time;  $\xi$ =lag distance;  $f_{Xi}(\xi)$ =probability density function of step length of the  $i$ -th fraction of the mixture; and a moving period during travelling a step length has been neglected. Meanwhile, the time derivative of  $V_i$  is expressed as follows:

$$\frac{\partial V_i(x,t)}{\partial t} = -E_i(x,t) + \int_0^{\infty} E_i(x-\xi,t) f_{Xi}(\xi) d\xi \quad (3)$$

By using the critical tractive force for each grain size, a pick-up rate formula proposed for uniform sand (Nakagawa & Tsujimoto (6)) could be applied to each grain size of graded bed material, as follows:

$$p_{si} \equiv p_{si} \sqrt{\frac{d_i}{(\sigma/\rho-1)g}} = F_0 \tau_{*i} \left(1 - \frac{k_2 \tau_{*ci}}{\tau_{*i}}\right)^m \quad (4)$$

in which  $\tau_{*i} \equiv u_*^2 / [(\sigma/\rho-1)gd_i]$ =dimensionless bed shear stress for each grain size;  $u_*$ =shear velocity;  $\sigma$ =density of sand;  $\rho$ =density of water;  $g$ =gravitational acceleration;  $\tau_{*c}$ =dimensionless critical tractive force; and the empirical constants are determined as follows:  $F_0=0.03$ ,  $k_2=0.7$  and  $m=3$  (Nakagawa & Tsujimoto (6)).

As for the critical tractive force for each grain size of sediment mixture,  $\tau_{*ci}$ , the following formula, derived by Egiazaroff (2) and slightly modified by Ashida & Michiue (1), is often adopted.

$$\frac{\tau_{*ci}}{\tau_{*cm}} = \left[ \frac{\ln 19}{\ln 19 \zeta_i} \right]^2 \quad (\text{for } \zeta_i > 0.4); \quad \frac{\tau_{*ci}}{\tau_{*cm}} = \frac{0.85}{\zeta_i} \quad (\text{for } \zeta_i \leq 0.4) \quad (5)$$

in which  $\zeta_i = d_i/d_m$ ;  $d_m$ =mean diameter; and  $\tau_{*cm}$ =dimensionless critical tractive force for sediment with the mean diameter in the mixture.  $\alpha_{cm} = \tau_{*cm}/\tau_{*c0}$  ( $\tau_{*c0}$  is the dimensionless critical tractive force for uniform bed material and it is almost 0.05 when the grain-size Reynolds number is larger than 100) is in general a function of the gradation of sediment mixture (8), but it is often assumed to be 1.0 conveniently or approximately.

According to an analytical work of Nakagawa et al. (8) and an empirical work of Parker et al. (9), Eq.5 might often overestimate the difference of critical tractive force due to sediment size, and the following approximation might represent the previous data more properly than Eq.5 as shown in Fig.3.

$$\frac{\tau_{*ci}}{\tau_{*cm}} = \left(\frac{d_i}{d_m}\right)^{-1} \quad (6)$$

With Eq.6, any fraction of sediment has the same critical tractive force, but it does not mean that an application of Eq.6 cannot succeed in an explanation of sorting including armoring and pavement formation.

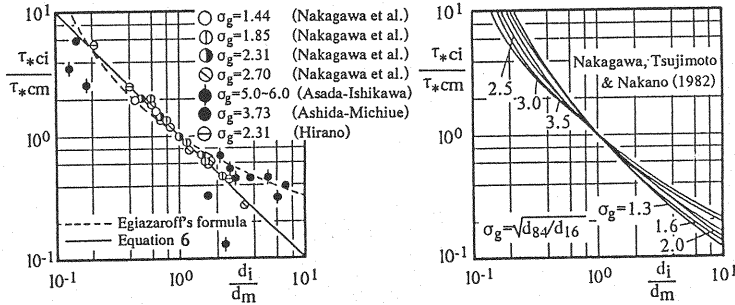


Fig.3 Critical tractive force for each grain size of sediment mixture

When Eq.6 is substituted into Eq.4, we succeed in prediction of pick-up rate for each grain size of sediment mixture as shown in Fig.4. Then, Eq.4 is rewritten as

$$p_{si} = F_0 \alpha_{cm} \tau_{*c0} \eta_m \left(1 - \frac{k_2}{\eta_m}\right)^m \left(\frac{d_i}{d_m}\right)^{-1} \quad (7)$$

in which  $\eta_m = \tau_{*m}/\tau_{*cm}$ ; and  $\tau_{*m} = u_*^2 / [(\sigma/\rho - 1)gd_m]$ . The following relation is deduced from Eq.7.

$$\frac{p_{si}}{p_{sm}} = \left(\frac{d_i}{d_m}\right)^{-1.5} \quad (8)$$

The step length for each grain size follows an exponential distribution on a flat bed, according to the experimental study by Nakagawa et al. (8). Hence, the probability density function of step length of the  $i$ -th fraction of the bed-load particles is written as

$$f_{Xi}(\xi) = \frac{1}{\Lambda_i} \exp\left(-\frac{\xi}{\Lambda_i}\right) \quad (9)$$

in which  $\Lambda_i$ =mean step length of the  $i$ -th fraction of bed load, and it is almost proportional to  $d_i$ .

$$\Lambda_i = \lambda d_i \quad (10)$$

According to the experiments by Nakagawa et al. (8),  $\lambda$  increases with the bed shear stress roughly from 10 to 50.

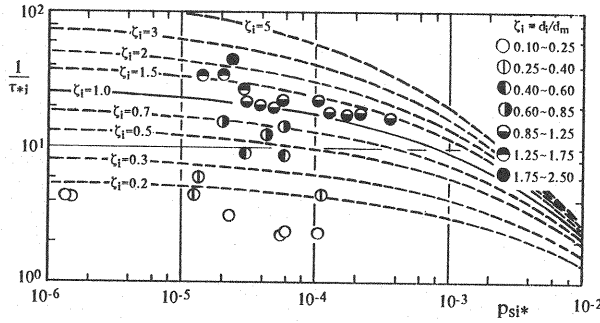


Fig.4 Pick-up rate for each grain size of sediment mixture

### FRACTIONAL TRANSPORT RATE ON A BED WITH LONGITUDINALLY ALTERNATE SORTING

In the following, the bed is idealized to be composed of two typical sizes,  $d$  and  $\beta d$  ( $\beta > 1$ ), and for convenience' sake, the former is simply called "sand"; while the latter "gravel". And a fluvial bed-surface with longitudinally alternate sorting is to be represented by sinusoidally varying  $p(x,t)$  written as

$$p(x,t) \equiv p_0[1 + \psi_p(x,t)] = p_0[1 + a \cdot \sin(kx - ct)] \quad (11)$$

in which  $p$ =volumetric ratio of gravel to the total bed materials in the bed-surface layer;  $p_0$ =volumetric ratio of gravel to the total bed materials in the substratum of the bed;  $p_0 a$ =amplitude of the fluctuation of  $p$ ;  $k$ =angular wave number; and  $c$ =propagation celerity.

The mean diameter of the bed-surface is assumed to be expressed as

$$d_m = [\beta p + (1-p)]d \quad (12)$$

Hence, the fluctuation of the mean diameter along the bed surface is expressed as

$$\frac{d_m}{d_{m0}} \equiv 1 + \psi_{dm} = 1 + \frac{p_0(1-\beta)}{p_0(1-\beta)+1} \psi_p \quad (13)$$

in which the subscript 0 indicates the values for the substratum or for the undisturbed bed-surface.

If the flow is assumed to be uniform, Manning-Strickler equation provides the following relation.

$$\frac{\tau_{*i}}{\tau_{*i0}} \equiv 1 + \psi_{Ti} = 1 + \frac{\psi_{dm}}{3} \quad (14)$$

The variation of the mean diameter along the bed surface changes the value of  $(d_i/d_m)$  for both sand and gravel, and thus the dimensionless critical tractive force for each grain size varies longitudinally. When Eq.6 is applied, the following equation is obtained.

$$\frac{\tau_{*ci}}{\tau_{*ci0m}} \equiv 1 + \psi_{Ci} = 1 + \psi_{dm} \quad (15)$$

The longitudinal variation of the pick-up rate is formally written as

$$\frac{p_{si}^*}{p_{si0}^*} \equiv 1 + \psi_{si} = 1 + \delta_{Ti} \psi_{Ti} + \delta_{Ci} \psi_{Ci} \quad (16)$$

in which  $\delta T_i$  and  $\delta C_i$  are obtained as follows when Eq.4 is applied.

$$\delta T_i \equiv \frac{\partial p_{sio*}}{\partial \tau_{*io}} \frac{\tau_{*io}}{p_{sio*}} = \frac{\eta_{m0} + (m+1)k_2}{\eta_{m0} - k_2} \quad (17)$$

$$\delta C_i \equiv \frac{\partial p_{sio*}}{\partial \tau_{*cio}} \frac{\tau_{*cio}}{p_{sio*}} = \frac{-mk_2}{\eta_{m0} - k_2} \quad (18)$$

in which  $\eta_{m0} \equiv \tau_{*m0}/\tau_{*cm0}$ . As seen from Eqs.14~18,  $\psi_s$  is related to  $\psi_p$  as follows irrespectively of sediment size.

$$\psi_s \equiv r_s \psi_p = \frac{\eta_{m0} - (2m+1)k_2}{3(\eta_{m0} - k_2)} \frac{p_0(\beta-1)}{p_0(\beta-1)+1} \psi_p \quad (19)$$

When  $\eta_{m0} > k_2$ , the bed is mobile.  $r_s$  becomes positive or negative depending on whether  $\eta_{m0}$  is larger or smaller than  $(2m+1)k_2$ . Hence, the variation of  $p_s(x,t)$  becomes in phase or out of phase with  $p(x,t)$ , independently of the sediment size.

When  $p(x,t)$  fluctuates, the volume of bed material for each grain size per unit area in the bed-surface layer,  $V_i$ , fluctuates as follows:

$$V_1(x,t) = V_{0p} = V_{10}(1+\psi_p) \quad (20)$$

$$V_2(x,t) = V_0(1-p) = V_{20}\left(1 - \frac{p_0\psi_p}{1-p_0}\right) \quad (21)$$

in which the subscripts 1 and 2 indicate the values for gravel and sand, respectively. Therefore, when the fluctuation of  $E_i(x,t)$  is expressed as

$$E_i(x,t) = E_{i0}(1+r_{Ei}\psi_p) \quad (22)$$

the following relations are obtained.

$$r_{E1} = r_s + 1; \quad r_{E2} = r_s - \frac{p_0}{(1-p_0)} \quad (23)$$

Both  $r_{E1}$  and  $r_{E2}$  become positive or negative, but the latter becomes negative more easily. It means that the fluctuation of the dislodged volume of sand from the bed ( $E_2(x,t)$ ) easily becomes out of phase for  $p(x,t)$ .

When  $E_i(x,t)$  is expressed by Eq.22 and the step length follows an exponential distribution as expressed by Eq.9, an application of Eq.2 clarifies the fluctuation of the fractional bed-load transport as follows:

$$q_{Bi}(x,t) = q_{Bi0}[1+r_{Bi}a \cdot \sin(\kappa x - ct - \phi_{Bi})] \quad (24)$$

in which

$$r_{Bi} = \frac{r_{Ei}}{\sqrt{1+(\kappa\Lambda_i)^2}}; \quad \sin\phi_{Bi} = \frac{\kappa\Lambda_i}{\sqrt{1+(\kappa\Lambda_i)^2}}; \quad \cos\phi_{Bi} = \frac{1}{\sqrt{1+(\kappa\Lambda_i)^2}} \quad (25)$$

The result implies that  $q_{Bi}(x,t)$  has a phase shift belonging to the first quadrature for  $E_i(x,t)$ , and its phase shift for gravel is larger than that for sand. This is qualitatively consistent with the measurements of the fractional bed-load discharge in the flumes by Ikeda & Iseya (3) and Kuhnle and Southard (5), but quantitative comparisons are irrelevant because the step length might be affected by bed-surface

condition of fully-developed diffuse gravel sheet. However, the above-mentioned analysis is still effective even quantitatively if it is applied to the initial small disturbance treated in a linear instability analysis.

### INSTABILITY OF LONGITUDINAL DISTURBANCE OF BED-SURFACE COMPOSITION

When the bed-surface composition is represented by the volumetric ratio of gravel to the total bed materials and it fluctuates as expressed by Eq.11, non-equilibrium bed-load transport brings the time variation of  $p(x,t)$ . Under a linear approximation, the time derivative of  $p$ ,  $\partial p/\partial t$ , is also expressed as a sinusoidal wave but with a phase shift, as follows:

$$\frac{1}{p_0} \frac{\partial p}{\partial t} = r_{pt} a \sin(\kappa x - ct - \phi_{pt}) \quad (26)$$

in which  $r_{pt} p_0 a$  and  $\phi_{pt}$  = amplitude and phase shift of the fluctuation of  $\partial p/\partial t$ , respectively. By comparing the direct time derivative of Eq.11 with Eq.26, the following relations are deduced.

$$\frac{1}{a} \frac{\partial a}{\partial t} = r_{pt} \cos \phi_{pt} ; \quad \kappa c = r_{pt} \sin \phi_{pt} \quad (27)$$

This implies that the amplification rate and the propagation celerity of the perturbation of bed-surface composition can be evaluated by  $r_{pt}$  and  $\phi_{pt}$ .

The time derivative of  $p$  is related to  $\partial V_i/\partial t$  as follows, after a linear approximation.

$$\frac{1}{p_0} \left( \frac{\partial p}{\partial t} \right) = \frac{1}{V_{10}} \frac{\partial V_1}{\partial t} - \frac{1}{V_0} \frac{\partial V}{\partial t} = (1-p_0) \left( \frac{1}{V_{10}} \frac{\partial V_1}{\partial t} - \frac{1}{V_{20}} \frac{\partial V_2}{\partial t} \right) \quad (28)$$

In a linearized mode,  $\partial V_i/\partial t$  can be also written by a sinusoidal wave as follows.

$$\frac{1}{V_{i0}} \left( \frac{\partial V_i}{\partial t} \right) = r_{v_{ti}} a \sin(\kappa x - ct - \phi_{v_{ti}}) \quad (29)$$

in which  $r_{v_{ti}} V_{i0} a$  and  $\phi_{v_{ti}}$  = amplitude and phase shift of the fluctuation of  $\partial V_i/\partial t$ , respectively. Then,  $r_{pt}$  and  $\phi_{pt}$  are related to  $r_{v_{ti}}$  and  $\phi_{v_{ti}}$ , as follows.

$$r_{pt}^2 = (1-p_0)^2 [r_{v_{t1}}^2 + r_{v_{t2}}^2 + 2r_{v_{t1}} r_{v_{t2}} (\cos \phi_{v_{t1}} \cos \phi_{v_{t2}} + \sin \phi_{v_{t1}} \sin \phi_{v_{t2}})] \quad (30)$$

$$r_{pt} \sin \phi_{pt} = (1-p_0) (r_{v_{t1}} \sin \phi_{v_{t1}} - r_{v_{t2}} \sin \phi_{v_{t2}}) \quad (31)$$

$$r_{pt} \cos \phi_{pt} = (1-p_0) (r_{v_{t1}} \cos \phi_{v_{t1}} - r_{v_{t2}} \cos \phi_{v_{t2}}) \quad (32)$$

Moreover, since  $\partial V_i/\partial t$  is related to  $E_i(x,t)$  by Eq.3 and  $E_i(x,t)$  is written as Eq.22, the following relations are deduced.

$$r_{v_{ti}} = \frac{\kappa \Lambda_i}{\sqrt{1 + (\kappa \Lambda_i)^2}} P_{sio} r_{Ei} \quad (33)$$

$$r_{v_{ti}} \sin \phi_{v_{ti}} = \frac{\kappa \Lambda_i}{\sqrt{1 + (\kappa \Lambda_i)^2}} P_{sio} r_{Ei} ; \quad r_{v_{ti}} \cos \phi_{v_{ti}} = - \frac{(\kappa \Lambda_i)^2}{\sqrt{1 + (\kappa \Lambda_i)^2}} P_{sio} r_{Ei} \quad (34)$$

By substituting Eqs.33 and 34 into Eqs.30~32,  $\phi_{pt}$  is determined.

As a result, the following equations are obtained.

$$M_* \equiv \frac{1}{(1-p_0)p_{s0}} \frac{1}{a} \left( \frac{\partial a}{\partial t} \right) = \frac{k_*^2}{1+k_*^2} (-\beta X + Y) \quad (35)$$

$$N_* \equiv \frac{\kappa c}{(1-p_0)p_{s0}} = \frac{k_*}{1+k_*^2} (X - Y) \quad (36)$$

in which

$$X \equiv \frac{1}{\sqrt{\beta}} \frac{1+k_*^2}{1+(\beta k_*)^2} (1+r_s); \quad Y \equiv r_s - \frac{p_0}{1-p_0} \quad (37)$$

$k_* \equiv \kappa \Lambda = 2\pi \Lambda / L$ ;  $L$ =wave length of longitudinally alternate sorting;  $\Lambda$ =mean step length of the finer material;  $p_{s0}$ =undisturbed pick-up rate of the finer material; and Eqs.8 and 23 have been applied herein. As for  $r_s$ , Eq.19 has been obtained.

$M_*$  and  $N_*$  are dimensionless amplification rate and propagation celerity, respectively; and they are expressed as a combination of  $\beta$ ,  $p_0$  (properties of the substratum of the bed);  $\eta_{m0}$  (hydraulic condition) and  $k_*$  (scale of the alternate sorting).

#### CRITERION OF FORMATION OF LONGITUDINALLY ALTERNATE SORTING AND PREDOMINANT WAVE LENGTH

Figure 5 shows examples of the calculated results of  $M_*$  and  $N_*$  against  $k_*$  with  $\beta$ ,  $p_0$  and  $\eta_{m0}$  as parameters, and this figure demonstrates a possibility of an unstable longitudinal disturbance of bed-surface composition propagating downstream. Fig.5 suggests that the longitudinally alternate sorting grows favorably under the condition slightly larger than the threshold of motion for bed material ( $\eta_{m0}=k_2$ ). By comparing the present analysis with the instability analysis as an explanation of sand wave formation (4, 6), unstable disturbance of bed-surface composition always migrates downstream and the instability of bed-surface composition can be explained purely by the "lag" due to bed-load motion.

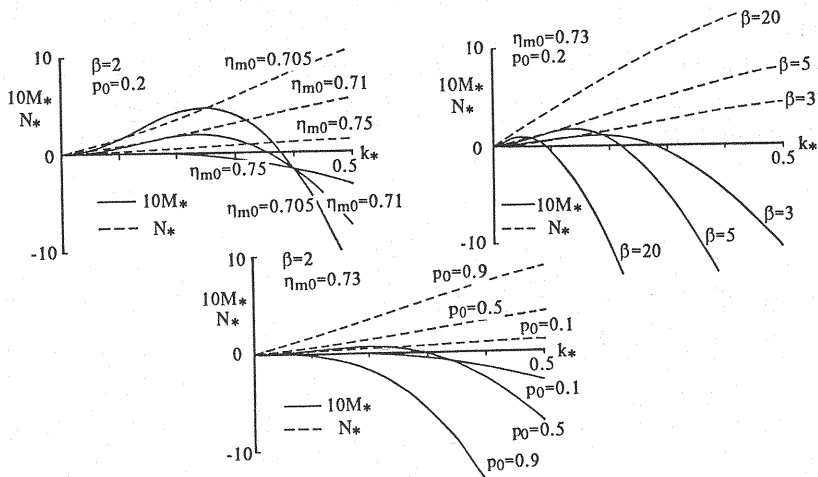


Fig.5 Dimensionless growth rate and propagation celerity of disturbance of bed-surface composition,  $M_*$  and  $N_*$

A predominant disturbance might be defined by the maximum growth rate ( $\partial a / \partial t \rightarrow \max$ ). Hence,  $\partial M_* / \partial k_* = 0$  provides the predominant wave number,  $\kappa_p$ .

In Fig.6, the dimensionless neutral and predominant wave numbers,  $k_{M*}$  and  $k_{P*}$ , are shown against  $p_0$  with  $\beta$  and  $\eta_{m0}$  as parameters. Similarly, the celerity of the predominant alternate sorting is calculated and is shown in Fig.7, in which the following dimensionless celerity is used.

$$c_* \equiv \frac{c}{\alpha_{cm} \sqrt{(\sigma/\rho - 1)gd}} = \frac{(1-p_0)p_{s0} \lambda N_*}{\alpha_{cm} k_*} \quad (38)$$

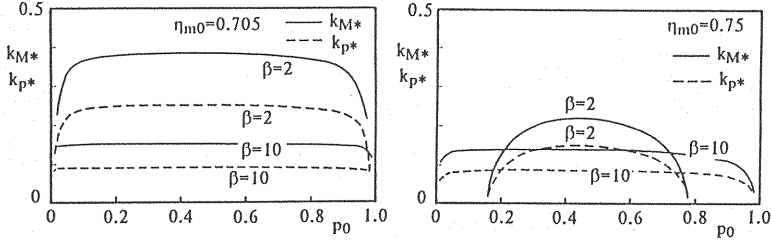


Fig.6 Dimensionless neutral and predominant wave numbers

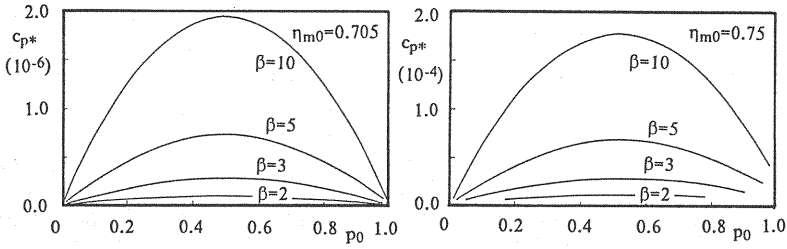


Fig.7 Propagation celerity of predominant disturbance

Figure 8 shows the contours of the maximum dimensionless bed shear stress  $\eta_{m0}$  where the bed-surface composition is longitudinally unstable on the  $\beta$ - $p_0$  plane under a given value of  $k_*$ . In general, near the critical condition of motion but in mobile beds, the longitudinal instability of bed-surface composition is easily promoted.

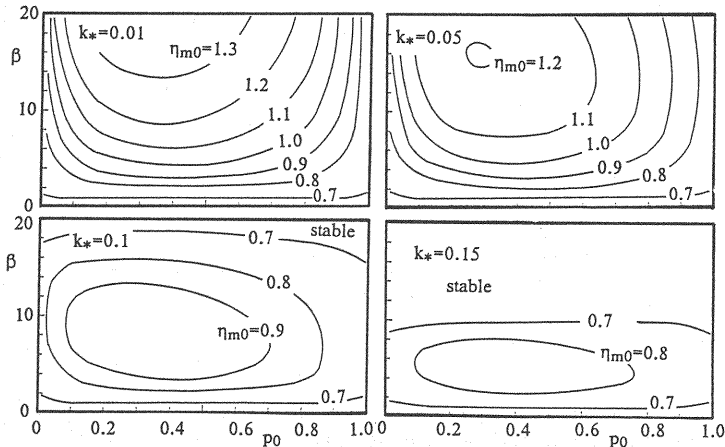


Fig.8 Contours of the maximum value of  $\eta_{m0}$  where bed-surface composition falls unstable



Moreover, the relation between the predominant wave length of longitudinally alternate sorting and the dimensionless bed shear stress is shown in Fig.9. By taking account of the fact that  $\Lambda$  is 10–20 times sand diameter, the predominant wave length of longitudinally alternate sorting is almost 500–1000 times diameter of the fine material, and it is roughly comparable with the length of small scale bed forms. The relation between the celerity and the bed shear stress is shown in Fig.10.

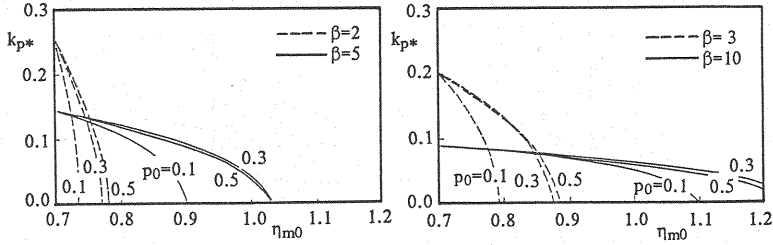


Fig.9 Relation between predominant wave number and bed shear stress

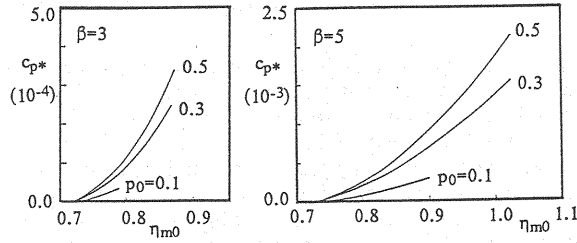


Fig.10 Relation between predominant wave celerity and bed shear stress

Although a comparison between the results of linear instability analysis and the observed data mostly concerned with the fully-developed states is rather irrelevant, such a comparison has been often performed also in the research works on sand wave formation. Conveniently or/and approximately, the present analytical results are also compared here with the observed data.

In Fig.11, the data obtained in an irrigation channel ( $B \approx 1.5\text{m}$ ;  $B$ =channel width) are compared with the theoretical results. The data were as follows: (1)  $d \approx 0.017\text{--}0.022\text{cm}$ ,  $\beta = 5\text{--}10$ ,  $p_0 = 0.16\text{--}0.25$ ,  $L = 12.7\text{cm}$ ,  $h = 10.8\text{cm}$  and  $\eta_{m0} \approx 0.705$ ; and (2)  $d \approx 0.02\text{--}0.03\text{cm}$ ,  $\beta = 5\text{--}8$ ,  $p_0 = 0.42\text{--}0.48$ ,  $L = 13.0\text{cm}$ ,  $h = 12.6\text{cm}$  and  $\eta_{m0} \approx 0.705$ . The value of  $\eta_{m0}$  for both cases was roughly estimated from the observation of the flow velocity, depth and the behavior of bed-load motion. The data exist in the range where longitudinally alternate sorting is expected to develop most actively (Fig.11(a)), and the observed wave length is well consistent with the theoretically predicted one (Fig.11(b)).

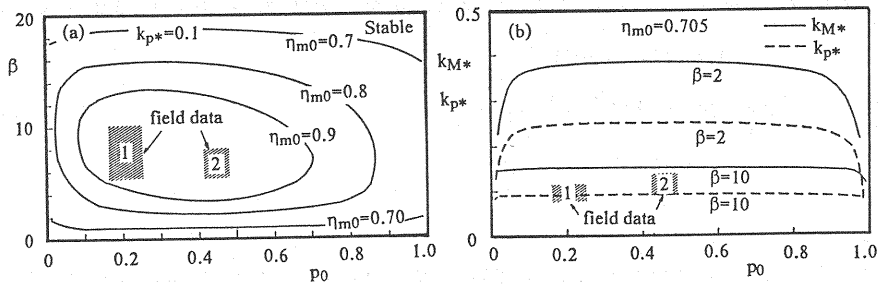


Fig.11 Comparison between the field data and the present theory

Besides them, the data of the flume experiments by Ikeda & Iseya (3) are also plotted in Fig.12. Although the experimental conditions were not necessarily obvious, roughly estimated conditions were

as follows:  $d=0.037\text{cm}$ ,  $\beta=7.03$ ,  $\eta_{m0}\approx 0.73$ ; and  $p_0=0.45$  for RUN I-1 and  $p_0=0.67$  for RUN I-2. RUN I-2 is well consistent with the theory but RUN I-1 is not. The writer feels that more data should be collected not only for comparisons as above mentioned but also in order to deepen our understanding of sorting process.

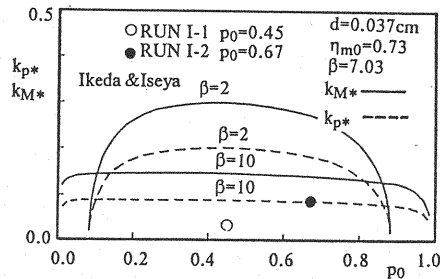


Fig.12 Comparison between the flume data (Ikeda & Iseya) and the present theory

## CONCLUSIONS

In a stream composed of sand and gravel, longitudinally alternate sorting is often observed. Such an alternate sorting is interesting from the view point of clarifying bed-load fluctuation as well as from the view point of understanding an instability of bed-surface composition due to selective and non-equilibrium transport of heterogeneous size material.

Bed-load transport model characterized by pick-up rate and step length for each grain size has been adopted, and basic equations to govern non-equilibrium transport and sorting process on the bed-surface have been deduced. Moreover, the constituent elements of the model have been investigated.

Based on the above-mentioned governing equations, the non-equilibrium transport on a bed with longitudinally alternate sorting has been analyzed in a linearized mode. As a result, fluctuations of fractional transport rates with different phase shifts have been deduced, and such an expected phenomenon is qualitatively consistent with the observations in laboratories, though a linear analysis cannot describe a fully-developed sorting bed quantitatively.

A linear theory is still effective to explain the incipient formation of alternate sorting just as similarly as it is successfully applied to explain sand wave formation. A small perturbation of the volumetric ratio of gravel to the total bed materials in the bed-surface layer has been assumed, and it has been inspected whether it grows or decays through non-equilibrium bed-load motion. As a result, an unstable condition of the perturbation propagating downstream certainly exists. Particularly under the hydraulic condition just above the threshold of motion of a bed-load particle, longitudinally alternate sorting is easily promoted to grow.

The maximum growth rate defines a predominant wave of sorting, and its wave length and celerity have been predicted.

Although the results by a linear analysis could not necessarily be applied to the fully-developed states as usually observed in flumes or streams, they used to be compared with the observed data conveniently or/and approximately. Such an attempt has been also done in this study, and the conformity of the theoretical results with the observation is fairly good, though more observations and measurements should be added in the future.

Most part of this paper is translated from the Japanese paper of the author published in Proc. of JSCE (11), though some parts are revised herein.

## ACKNOWLEDGEMENTS

The author was much interested in the presentation of the paper by Ikeda & Iseya (3) where they reported an observation of a streamwise migration of alternation of finer and coarser parts, and a profitable discussion with Prof. Gary Parker (Minnesota University) about sorting process became a key by which the author started the present analysis. When Dr. Roger A. Kuhnle (U.S. Department of Agriculture) came to Japan at the 6th APD-IAHR Congress held in Kyoto, he explained about gravel sheets observed in his laboratory, and the author convinced that the present analysis was consistent with the actual phenomenon. On computations in the analysis and the field observation, Mr. Ken Motohashi

(Nihon Suido Consultants; formerly a graduate student, Kanazawa University) helped the author very much. The author expresses sincere gratitude to those who helped this study directly and indirectly.

## REFERENCES

1. Ashida, K. and M. Michiue : Studies on bed load transportation for nonuniform sediment and river bed variation. *Annals of the Disaster Prevention Research Institute*, Kyoto University, No.14B, pp.259-273, 1971 (in Japanese).
2. Egiazaroff, I.V. : Calculation of nonuniform sediment concentration. *Journal of the Hydraulics Division*, ASCE, Vol.91, No.HY4, pp.73-80, 1965.
3. Ikeda, H. and F. Iseya : Longitudinal sorting process in heterogeneous sediment transportation. *Proc. 30th Japanese Conference on Hydraulics*, JSCE, pp.217-222, 1986 (in Japanese).
4. Kennedy, J.F. : The mechanics of dunes and antidunes in erodible-bed channels. *Journal of Fluid Mechanics*, Vol.16, Part 4, pp.521-544, 1963.
5. Kuhnle, R.G. and J. Southard : Bed load transport fluctuations in a gravel bed laboratory channel. *Water Resources Research*, Vol.24, No.2, pp.247-260, 1988.
6. Nakagawa, H. and T. Tsujimoto : Sand bed instability due to bed load motion. *Journal of the Hydraulics Division*, ASCE, Vol.106, No.HY12, pp.2029-2051, 1980.
7. Nakagawa, H., T. Tsujimoto and T. Hara : Armoring in alluvial bed composed of sediment mixtures. *Annals of the Disaster Prevention research Institute*, Kyoto University, No.20B-2, pp.355-370, 1977 (in Japanese).
8. Nakagawa, H., T. Tsujimoto and S. Nakano : Characteristics of sediment motion for respective grain sizes of sediment mixtures, " *Bulletin of the Disaster Prevention Research Institute*, Kyoto University, Vol.32, pp.1-32, 1982.
9. Parker, G., P.C. Klingeman and D.G. McLean : Bedload and size distribution in paved gravel-bed streams. *Journal of the Hydraulics Division*, ASCE, Vol.108, No.HY4, pp.544-571, 1982.
10. Tsujimoto, T. : Longitudinal stripes of alternate lateral sorting due to cellular secondary currents, " *Proc. 23rd IAHR Congress*, Vol.2, Ottawa, Canada, pp.17-24, 1989.
11. Tsujimoto, T. : Formation of alternate longitudinal sorting as an instability of fluvial bed-surface composition. *Proc. JSCE*, No.411/II-12, pp.143-150, 1989 (in Japanese).

## APPENDIX -NOTATION

The following symbols are used in this paper:

$a$	= amplitude of perturbation of $p$ ;
$c, c_*$	= propagation celerity of perturbation of bed-surface composition and its dimensionless expression;
$d$	= diameter of sand (fine material);
$d_i, d_m$	= diameter of the $i$ -th fraction material; mean diameter;
$E_i$	= substantial volume of the $i$ -th fraction material dislodged from a bed per unit time per unit area;
$f_{Xi}(x)$	= probability density function of step length of the $i$ -th fraction of sediment mixture;
$F_0$	= constant in pick-up rate formula;
$g$	= gravitational acceleration;
$h$	= flow depth;
$k_2$	= constant in pick-up rate formula;
$k_*$	= dimensionless wave number ( $\equiv k\Lambda$ );
$k_{M*}, k_{p*}$	= dimensionless neutral and predominant wave number;
$L$	= wave length;
$m$	= constant in pick-up rate formula;
$M_*$	= dimensionless growth rate of perturbation;

$N_*$	= dimensionless propagation celerity of perturbation;
$p$	= volumetric ratio of gravel to the total bed materials in bed-surface layer;
$p_0$	= volumetric ratio of gravel to the total bed materials in the substratum of the bed;
$p_i$	= volumetric ratio of the $i$ -th fraction material to the total bed materials in bed-surface layer;
$p_s$	= pick-up rate of sand (fine material);
$p_{si}$	= pick-up rate of the $i$ -th fraction of sediment mixture;
$q_{Bi}$	= fractional bed-load transport rate;
$r_{Ei}$	= dimensionless amplitude of perturbation of $E_i$ ;
$r_{pt}, r_{vti}$	= dimensionless amplitudes of $\partial p/\partial t$ and $\partial V_i/\partial t$ ;
$r_s$	= dimensionless amplitude of perturbation of pick-up rate;
$u_*$	= shear velocity;
$V_i$	= substantial volume of the $i$ -th fraction material in bed-surface layer per unit area;
$V$	= total substantial volume of material in bed-surface layer per unit area;
$\alpha_{cm}$	$\equiv \tau_{*cm}/\tau_{*c0}$ ;
$\beta$	= ratio of diameter of gravel (coarse material) to that of sand (fine material);
$\delta_{Ci}, \delta_{Ti}$	= defined by Eqs.17 and 18, respectively;
$\zeta_i$	= $d_i/d_m$ ;
$\eta_m$	= $\tau_{*m}/\tau_{*cm}$ ;
$\theta_E$	= thickness of bed-surface layer;
$\kappa$	= angular wave number;
$\lambda$	= dimensionless mean step length ( $\equiv \Lambda_i/d_i$ );
$\Lambda$	= mean step length of sand (fine material);
$\Lambda_i$	= mean step length of the $i$ -th fraction of sediment mixture;
$\rho, \sigma$	= mass density of fluid; mass density of sediment;
$\rho_0$	= porosity of bed material;
$\tau_{*c0}$	= dimensionless critical tractive force for uniform bed material;
$\tau_{*ci}, \tau_{*cm}$	= dimensionless critical tractive force for each grain size; dimensionless critical tractive force for sediment with mean diameter in sediment mixture;
$\tau_{*i}$	= dimensionless tractive force for each grain size ( $\equiv u_*^2/[(\sigma/\rho-1)gd_i]$ );
$\phi_{Bi}$	= phase shift of $q_{Bi}(x,t)$ from $p(x,t)$ ;
$\phi_{pt}, \phi_{vti}$	= phase shifts of $\partial p/\partial t$ and $\partial V_i/\partial t$ from $p(x,t)$ ;
$\psi_{dm}, \psi_p$	= dimensionless perturbations of $d_m$ and $p$ ; and
$\psi_{Ci}, \psi_{Ti}, \psi_{si}$	= dimensionless perturbations of $\tau_{*ci}, \tau_{*i}$ and $p_{si}$ .

### Subscripts

$0$	= undisturbed bed-surface or substratum of the bed;
$i$	= $i$ -th fraction material;
$m$	= mean diameter;
$p$	= predominant wave with the maximum growth rate of sorting; and
$pt, vti$	= $\partial p/\partial t$ and $\partial V_i/\partial t$ .